Policy Research Journal
ISSN (E): 3006-7030 ISSN (P) : 3006-7022 Volume 4, Issue 3, 2026

PHOTOREDOX CATALYZED C-N BOND FORMATION USING VISIBLE LIGHT FOR SUSTAINABLE SYNTHESIS OF NITROGEN HETEROCYCLES

Muhammad Faisal Asghar[*1], Imran Hussain[2], Talha[3]

[*1]*(M. phil chemistry) University of Agriculture, Faisalabad*
[2]*University: Allama Iqbal Open University Islamabad, Balochistan Pakistan*
[3]*Universiy of Makram*

[*1]faysalasghar902@gmail.com, [2]himran873@gmail.com, [3]talha@uomp.edu.pk

DOI: https://doi.org/10.5281/zenodo.23557544

Keywords
Photoredox catalysis; visible light; C–N bond formation; nitrogen heterocycles; metallaphotoredox; green chemistry; sustainable synthesis; nitrogen-centered radicals

Article History
Received: 07 January 2026
Accepted: 17 March 2026
Published: 31 March 2026

Copyright @Author
Corresponding Author: *
Muhammad Faisal Asghar

Abstract

Nitrogen-containing heterocycles constitute the structural cornerstone of modern medicinal chemistry, featuring in over 84% of FDA-approved small-molecule therapeutics. Traditional methodologies for constructing carbon–nitrogen (C–N) bonds, including Buchwald–Hartwig, Ullmann, and Chan–Lam couplings, rely on elevated temperatures, stoichiometric strong bases, and precious-metal catalysts, resulting in poor functional group tolerance, heavy-metal contamination, and elevated environmental metrics. Visible-light photoredox catalysis has emerged as a transformative paradigm, harnessing abundant photon energy to drive single-electron transfer (SET) and energy transfer (EnT) processes under ambient conditions. This review provides a comprehensive analysis of visible-light-driven photoredox-catalyzed C–N bond formation for the sustainable synthesis of nitrogen heterocycles. Fundamental photophysical and electrochemical principles governing photocatalyst design are examined, including excited-state redox potentials, triplet lifetimes, and quenching cycles. The review systematically compares pure organophotoredox protocols employing organic dyes such as 4CzIPN, Eosin Y, and acridinium salts against dual metallaphotoredox systems utilizing Earth-abundant nickel, copper, and cobalt co-catalysts. Mechanistic pathways for generating nitrogen-centered radicals aminyl, amidyl, iminyl, and carbamoyl species via direct SET, proton-coupled electron transfer (PCET), and homolytic N–X cleavage are discussed, alongside radical cyclization cascades yielding privileged scaffolds including indoles, quinolines, imidazoles, and pyrazoles. Quantitative green chemistry metrics Atom Economy, E-Factor, and Process Mass Intensity demonstrate that photoredox methodologies substantially outperform classical thermal coupling routes, eliminating precious metals, reducing energy demand, and minimizing waste. Emerging horizons including microfluidic continuous-flow photoreactors, electrophotocatalysis, heterogeneous recyclable platforms, and Earth-abundant metal catalysis are highlighted as pathways toward industrial adoption.

1. INTRODUCTION

Nitrogen-containing heterocycles represent a cornerstone of organic and medicinal chemistry, serving as the core pharmacophores in over 84% of U.S. Food and Drug Administration (FDA)-approved small-molecule therapeutics, as well as a broad spectrum of agrochemicals, natural products, and materials sciences (Vitaku et al., 2014). Among these privileged architectures, indoles, quinolines, imidazoles, and pyrazoles possess diverse biological profiles, ranging from antimicrobial and anti-inflammatory activities to complex oncological targets. Consequently, the development of efficient, chemo- and regioselective methodologies for the construction of carbon-nitrogen (C-N) bonds remains a primary objective in modern synthetic methodology (Feng et al., 2024).

For decades, the synthesis of nitrogen heterocycles and the image-arylation or image-alkylation of structural building blocks relied heavily on traditional thermochemical cross-coupling protocols. Classic amination reactions most notably the Buchwald-Hartwig, Ullmann, and Chan-Lam couplings revolutionized industrial chemical manufacturing by enabling direct bond formation between nitrogen nucleophiles and aryl halides or boronic acids (Dorel et al., 2019). However, these thermochemical processes frequently require elevated reaction temperatures (image), stoichiometric amounts of strong, non-nucleophilic bases (e.g., sodium *tert*-butoxide, potassium phosphate), and precious platinum-group metal catalysts (e.g., palladium, iridium) paired with intricate, air-sensitive phosphine or carbene ligands. These aggressive conditions introduce severe operational limitations, including poor functional group tolerance for base- or heat-sensitive substrates, substantial heavy-metal contamination, high Process Mass Intensity (PMI), and elevated Environmental Factors (E-Factors) (Beletskaya & Averin, 2021).

Visible-light photoredox catalysis has emerged as a transformative paradigm to address these synthetic bottlenecks. By utilizing visible light (image) as a clean, abundant energy source, photoredox catalysts can convert low-energy single photons into chemical potential via Single Electron Transfer (SET) or Energy Transfer (EnT) manifolds under ambient conditions (Prier et al., 2013). Excited-state photosensitizers engage with organic substrates or secondary transition-metal complexes to generate highly reactive open-shell intermediates such as aminyl radicals, aminium radical cations, and carbon-centered radical precursors under mild, redox-neutral conditions. This operational mildness minimizes side reactions, streamlines step economy by facilitating direct C-H and N-H functionalization, and drastically reduces the energy demand of heterocyclic synthesis (Zhao & Xia, 2018).

This review provides a comprehensive analysis of visible-light-driven photoredox-catalyzed C-N bond formation for the sustainable construction of nitrogen heterocycles. It encompasses fundamental photophysical principles, organophotoredox versus metallaphotoredox dual catalysis, detailed mechanistic radical cascades yielding specific privileged heterocycles, and quantitative green chemistry evaluations comparing photoinduced methodologies against classic thermal coupling routes (Sinha et al., 2025).

2. Photophysical and Electrochemical Foundations of Photoredox Catalysis

The operational efficacy of a photoredox transformation depends on the underlying photophysical and electrochemical properties of the photosensitizer. Upon irradiation with visible light, ground-state photocatalyst molecules (PC) absorb photons corresponding to their maximum absorption wavelength (λ_{max}), promoting an electron from the Highest Occupied Molecular Orbital (HOMO) to the Lowest Unoccupied Molecular Orbital (LUMO) to yield a short-lived singlet excited state ($^1PC^*$). Rapid intersystem crossing (ISC), facilitated by strong spin-orbit coupling, populates a lower-energy, long-lived triplet excited state ($^3PC^*$) (Chen et al., 2016).

The triplet excited species ($^3PC^*$) possesses thermodynamic amphotericity: it acts simultaneously as a stronger single-electron oxidant and a stronger single-electron reductant than the ground-state species (PC). The

thermodynamic driving force for electron transfer is governed by the excited-state redox potentials, calculated via the Rehm-Weller approximation:

$$E_{1/2}(PC^*/PC^{\cdot-}) = E_{1/2}(PC/PC^{\cdot-}) + E_{0,0}$$
$$E_{1/2}(PC^{\cdot+}/PC^*) = E_{1/2}(PC^{\cdot+}/PC) - E_{0,0}$$

where $E_{0,0}$ represents the zero-zero spectroscopic transition energy between the ground and lowest excited states (Yang et al., 2023).

Photoredox catalysis operates through two distinct single-electron pathways:

- **Oxidative Quenching Cycle**: The excited state PC^* donates an electron to an electron-accepting substrate or additive (A), yielding a reduced substrate radical anion ($A^{\cdot-}$) and an oxidized catalyst species ($PC^{\cdot+}$). The ground state PC is subsequently regenerated when $PC^{\cdot+}$ accepts an electron from an electron donor (D), producing an oxidized species ($D^{\cdot+}$).
- **Reductive Quenching Cycle**: The excited state PC^* accepts an electron from an electron-donating substrate or sacrificial reductant (D), generating an oxidized substrate radical cation ($D^{\cdot+}$) and a reduced catalyst species ($PC^{\cdot-}$). Subsequent electron transfer from $PC^{\cdot-}$ to an electron acceptor (A) restores the ground-state photocatalyst PC (Corrigan et al., 2016).

In addition to SET, photocatalysts can operate through Energy Transfer (EnT) via Dexter-type triplet-triplet energy transfer. In this mechanism, non-radiative exchange of electron spins occurs between $^3PC^*$ and a ground-state substrate (S_0), promoting the substrate to its reactive triplet state ($S_1 \rightarrow T_1$) without net charge exchange (ΔE_{TT}) (Kabir & Uzzaman, 2022).

To select appropriate photocatalysts for C-N bond-forming reactions, synthetic chemists evaluate excited-state lifetimes (τ), redox potentials, molar extinction coefficients (ϵ), and photostability. Polypyridyl complexes of iridium (III) and ruthenium (II), such as $[Ru(bpy)_3]^{2+}$ and $[Ir(ppy)_3]$, served as foundational photocatalysts due to their long triplet lifetimes and high quantum yields. However, the drive toward sustainable process chemistry has accelerated the adoption of metal-free organic photoredox catalysts (e.g., 4CzIPN, Eosin Y, acridinium salts) and heterogeneous organic frameworks (Heravi et al., 2018).

IEER
Institute for Excellence in Education & Research

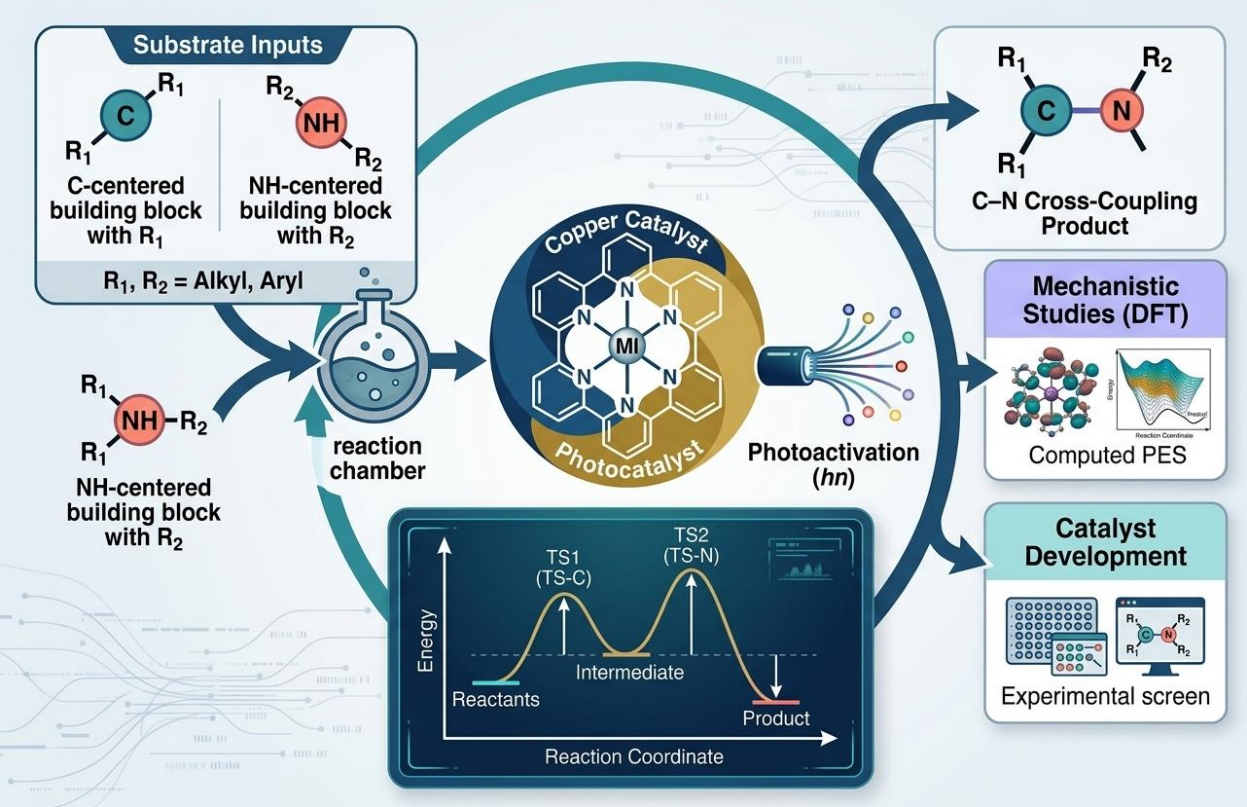


Figure 2: Overview of Light-Activated Copper Metallaphotoredox C–N Cross-Coupling, Reaction Energy Landscapes, and Experimental Screening Workflows.

Table 1: Photophysical and Electrochemical Properties of Representative Photocatalysts

Photocatalyst Class	Catalyst Name	Absorption λmax (nm)	Excited State Lifetime (τ)	E1/2 (PC∗/PC·−) (V vs. SCE)	E1/2 (PC·+/PC∗) (V vs. SCE)	Primary Reaction Pathway
Ru-Polypyridyl	$[Ru(bpy)_3]^{2+}$	452	1100 ns	+0.77	-0.81	SET (Reductive/Oxidative)
Ir-Polypyridyl	$Ir(ppy)_3$	375	1900 ns	+0.31	-1.73	SET (Oxidative) / EnT
Organic D-A	4CzIPN	375 / 470	5100 ns	+1.35	-1.04	SET / Dual Metallaphotoredox
Xanthene Dye	Eosin Y	542	1700 ns	+0.83	-1.14	SET (Reductive) / HAT
Acridinium Dye	Mes-Acr-Me^+	425	5–15 ns	+2.06	-0.57	Direct Strong SET Oxidation

Analysis of these parameters reveals key design trade-offs. Organophotoredox catalysts like Mes-Acr-Me^+ offer strong oxidizing potentials (+2.06 V vs. SCE) capable of oxidizing unfunctionalized, electron-deficient anilines; however, their short excited-state lifetimes (τ =

5–15 ns) demand higher substrate concentrations to ensure efficient diffusional quenching. Conversely, carbazolyl dicyanobenzene donor-acceptor dyes, such as 4CzIPN, combine high excited-state reduction potentials ($+1.35$ V vs. SCE) with microsecond triplet lifetimes ($\tau = 5.1\ \mu$s), making them effective organic replacements for precious metal complexes in dual catalytic cross-couplings (Yadav et al., 2024).

3. Catalytic Paradigms in Visible Light-Driven C-N Bond Formation

Visible light-induced C-N bond formation can be divided into two primary catalytic regimes: pure organophotoredox systems and dual metallaphotoredox systems (Kancherla et al., 2019).

3.1 Pure Organophotoredox Protocols

Purely organophotoredox strategies operate without transition metal co-catalysts, utilizing organic dyes to promote transformations through direct SET or Hydrogen Atom Transfer (HAT) steps. Direct single-electron oxidation of neutral primary or secondary amines yields an aminium radical cation intermediate ($R_2NH^{+\cdot}$), which exhibits significantly enhanced $N-H$ acidity. Subsequent deprotonation delivers a neutral, nitrogen-centered aminyl radical ($R_2N^{\cdot}$) that can undergo intramolecular cyclization onto tethered unsaturated moieties or intermolecular addition to radical traps (O'Brien et al., 2023).

A prominent organophotoredox organocatalytic framework involves organo-dyes such as *N*-hydroxyphthalimide (NHPI). Under irradiation, NHPI can undergo photoinduced oxidation to form the phthalimide *N*-oxyl (PINO) radical, a species capable of driving abstraction of weak $C(sp^3)-H$ bonds adjacent to nitrogen atom centers. This HAT step generates α-aminoalkyl radicals, enabling formal [4+1] and [3+2] radical annulments to form fused heterocyclic cores (Cybularczyk-Cecotka et al., 2020).

3.2 Metallaphotoredox Dual Catalysis

While organophotoredox catalysis excels at generating native open-shell species via $C-H$ or $N-H$ activation, it often struggles to promote direct cross-coupling between two distinct aryl or alkyl nucleophile/electrophile pairings. Metallaphotoredox catalysis overcomes this limitation by pairing an organic or inorganic photoredox cycle with a transition metal catalytic cycle (typically nickel, copper, cobalt, or iron) (Ni et al., 2026).

In a representative dual nickel/photoredox C-N cross-coupling manifold, the transition metal center serves as the site for $C-N$ bond construction via multi-valent oxidation states, while the photoredox catalyst regulates the oxidation state of the nickel complex through single-electron transfers. The transformation initiates with oxidative addition of a low-valent Ni^0 complex into an aryl halide ($Ar-X$), generating an $Ar-Ni^{II}-X$ intermediate. Coordination of an amine nucleophile followed by deprotonation yields an $Ar-Ni^{II}-NR_2$ complex (Ghosh et al., 2026). At this junction, the excited-state photocatalyst ($*PC$) oxidizes the $Ar-Ni^{II}-NR_2$ species via SET (or captures an in situ generated *N*-centered radical), affording a high-valent $Ar-Ni^{III}-NR_2$ species. This transient Ni^{III} complex undergoes rapid reductive elimination to construct the desired $C-N$ bond and extrude a Ni^{I} complex, overcoming the high activation energy barrier ($\Delta G^{\ddagger}$) associated with reductive elimination from lower-valent Ni^{II} amido intermediates. Finally, the reduced photocatalyst ($PC^{\cdot-}$) donates an electron to the Ni^{I} species via a second SET, regenerating both ground-state catalysts (PC and Ni^0) simultaneously (Dow, 2023).

Innovations in this field include base-free and ligand-free metallaphotoredox aminations. For instance, primary alkylamines such as *tert*-butylamine (*t*-BuNH_2) can serve simultaneously as the nitrogen nucleophile, proton acceptor, and transient stabilizing ligand for Ni^{II} intermediates, simplifying reaction formulations and improving process mass intensity (Goldschmid, 2025).

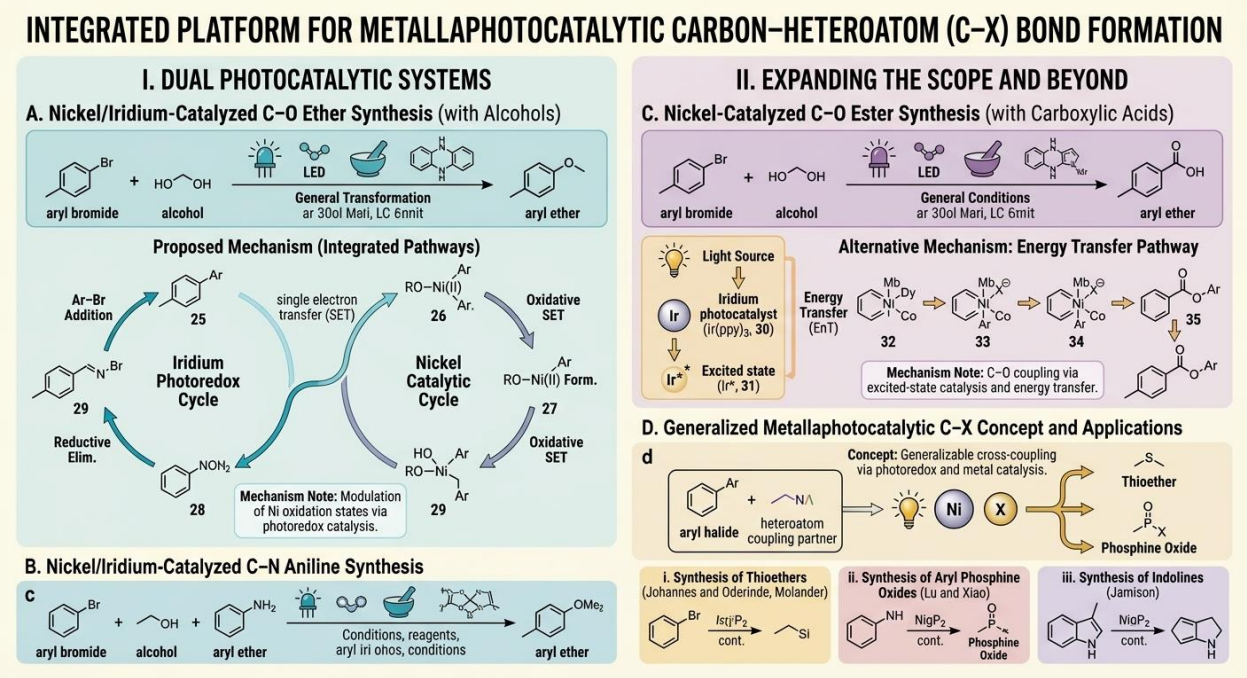


Figure 1: Mechanistic Manifolds and Applications of Integrated Dual Nickel/Photoredox Cross-Coupling Pathways for Carbon–Heteroatom (C–X) Bond Formation.

Table 2: Comparison of Catalytic Systems in Visible-Light C-N Coupling

Catalytic System	Representative Catalytic Combination	Primary Mechanism	Typical Substrate Scope	Key Operational Advantages
Metal-Free Organophotoredox	4CzIPN or Mes-Acr-Me$^+$ (0.5–2 mol%)	Direct SET / Radical Cation Formation	Electron-rich Anilines, Amides, N-Alkylamines	Zero heavy-metal contamination; low cost; tolerant of air/moisture
Dual Ni/Photoredox	$NiBr_2$·glyme (5 mol%) + 4CzIPN (0.5 mol%)	Synergistic $Ni^0/Ni^{II}/Ni^{III}$ redox-gated coupling	Aryl Bromides/Iodides + Primary/Secondary Amines	Operates at 25°C; mild bases; high yields with unactivated nucleophiles
Dual Cu/Photoredox	CuCl / $Cu(OAc)_2$ + $[Ru(bpy)_3]^{2+}$ or Organic Dyes	Photo-assisted copper radical cross-coupling	Alkyl Halides, Carboxylic Acids (Decarboxylative), Amines	High chemoselectivity for C(sp^3)–N bond formation; scalable
Heterogeneous Photocatalysis	Ru-doped ZnO or Porous Organic Polymers (POPs)	Surface-bound SET / Interfacial Electron Transfer	N-Heteroaromatics, Indoles, Sulfonamides	Catalyst recovery via simple filtration; reusable over >6 cycles

4. Mechanistic Pathways for Radical-Mediated Nitrogen Heterocycle Synthesis

The construction of complex nitrogen heterocycles via visible-light photoredox catalysis typically proceeds through radical-mediated cyclization cascades. Understanding these reaction mechanisms requires analyzing how nitrogen-centered radicals (NCRs) are generated and how they react with unsaturated functional groups (Chen et al., 2016).

4.1 Generation and Reactivity of Nitrogen-Centered Radicals (NCRs)

Nitrogen-centered radicals can be classified into aminyl ($R_2N^{\cdot}$), aminium radical cations ($R_2NH^{+\cdot}$), amidyl ($R-CO-NR^{\cdot}$), iminyl ($R_2C=N^{\cdot}$), and carbamoyl radicals based on their electronic structures and oxidation states. Three primary synthetic pathways are used to generate these species under photoredox conditions:

1. **Direct SET Oxidation/Deprotonation**: An electron-rich amine undergoes single-electron oxidation by an excited photocatalyst ($*PC$), yielding an aminium radical cation ($R_2NH^{+\cdot}$). The significant drop in pK_a (often by $> 15\ pK_a$ units) enables rapid deprotonation by weak, ambient bases, yielding a neutral aminyl radical ($R_2N^{\cdot}$) (Wang et al., 2026).
2. **Proton-Coupled Electron Transfer (PCET)**: In systems where direct SET oxidation is thermodynamically unfavorable, a multisite PCET pathway can be employed. Here, a hydrogen-bonded base abstracts the $N-H$ proton simultaneously as the excited photosensitizer accepts an electron, bypassing high-energy charged intermediates and enabling direct generation of neutral aminyl radicals (Liang et al., 2024).
3. **Homolytic Cleavage of Pre-activated N-X Bonds**: Substrates bearing weak $N-O$ (e.g., O-benzoyl hydroxylamines), $N-N$, or $N-X$ bonds can accept an electron from a reduced photocatalyst ($PC^{\cdot-}$), driving mesolytic cleavage to release a nitrogen radical and an anionic leaving group (Azzi et al., 2026).

4.2 Radical Cyclization Cascades

Once generated, NCRs undergo rapid intramolecular addition across tethered alkenes, alkynes, or arenes. Intramolecular additions generally follow Baldwin's rules for ring closure, with $5-exo-trig$ and $6-endo-trig$ cyclizations being kinetically favored for five- and six-membered ring formation, respectively. The resulting carbon-centered radical intermediate undergoes aromatization via oxidative single-electron transfer followed by deprotonation, or captures a second coupling partner in a multicomponent cascade (Gilmore & Alabugin, 2011).

4.3 Synthesis of Privileged Nitrogen Heterocycles Indoles and Indole Derivatives

Indoles represent a key heterocyclic framework in medicinal chemistry. Visible-light photoredox strategies allow access to substituted indoles through direct image activation of 2-vinylarylamines. For example, utilizing a 3,6-bis(trifluoromethyl)-functionalized phenanthrenequinone (image) photocatalyst paired with a cobaloxime dual catalyst under an inert atmosphere enables oxidative cyclization via neutral aminyl radicals (Zard, 2008). The photoredox catalyst initiates oxidation of the aniline nitrogen to form an aminyl radical, which undergoes a favorable image cyclization onto the pendant alkene. The resulting radical intermediate is subsequently oxidized and deprotonated by the cobaloxime co-catalyst, regenerating the double bond and yielding the aromatic indole core (Talvitie et al., 2025). This dual photoredox/cobaloxime architecture suppresses over-oxidation side reactions, delivering substituted indoles in high yields (image) without requiring stoichiometric chemical oxidants. Alternatively, organophotoredox-catalyzed oxidation of 3-(benzylidene) indolines yields functionalized indole-3-carbinols through radical cation intermediate pathways (Ghosh et al., 2025).

Quinolines and Tetrahydroquinolines

Quinolines are traditionally synthesized via condensation reactions (e.g., Skraup, Doebner, or Povarov protocols) that rely on harsh acid catalysts. Visible-light photoredox catalysis enables radical Povarov multi-component cyclizations under mild conditions. Irradiation of anilines and electron-rich alkenes (or alkynes) in the presence of an organophotoredox catalyst drives single-electron oxidation of the in situ formed imine, generating an iminium radical cation intermediate. Subsequent [4+2] formal cycloaddition with the alkene partner followed by re-aromatization yields quinolines or tetrahydroquinolines with high regiochemistry and broad functional group compatibility (Chadha & Silakari, 2017).

Imidazoles and Pyrazoles

Five-membered di-aza heterocycles, such as pyrazoles and imidazoles, can be synthesized via photoinduced cascade reactions. Photoredox-catalyzed [4+1] radical cyclizations between N-methylanilines and isocyanides mediated by NHPI or acridinium photocatalysts generate 3-iminodihydroindoles and imidazole derivatives at room temperature. The transformation proceeds through $C(sp^3) - H$ activation of the N-methyl group to form an α-aminoalkyl radical, which adds to the isocyanide carbon, followed by intramolecular cyclization onto the aromatic ring and subsequent re-aromatization (Kumari & Singh, 2019).

5. Green Chemistry Metrics and Sustainability Evaluation

Evaluating visible-light photoredox C-N coupling reactions against traditional thermochemical methodologies requires a quantitative analysis using standardized green chemistry metrics. Key metrics include Atom Economy (AE), Environmental Factor (E-Factor), and Process Mass Intensity (PMI) (Borah et al., 2026).

5.1 Mathematical Formulations of Sustainability Metrics

Atom Economy (AE)

Atom economy measures the proportion of reactant atoms incorporated into the final desired product:

$$\text{AE} = \left(\frac{\text{Molecular Weight of Desired Product}}{\sum \text{Molecular Weights of All Reactants}}\right) \times 100\%$$

Photoredox processes operating via direct $C - H$ or $N - H$ functionalization display high atom economy ($\text{AE} > 80\text{–}90\%$) because they avoid halogenation or leaving-group pre-functionalization steps (Salah, 2025).

Environmental Factor (E-Factor)

The E-Factor quantifies the total mass of waste generated per unit mass of product:

$$\text{E-Factor} = \frac{\text{Total Mass of Waste (kg)}}{\text{Mass of Desired Product (kg)}}$$

In industrial pharmaceutical manufacturing, target E-Factors for fine chemical synthesis typically range between 25 and > 100. Photoredox C-N couplings significantly lower E-Factors by eliminating stoichiometric metallic reagents, high-boiling toxic solvents, and halogenated waste (Lee et al., 2025).

Process Mass Intensity (PMI)

PMI measures the total mass of materials including reactants, catalysts, solvents, and purification reagents required to produce a given mass of product:

$$\text{PMI} = \frac{\text{Total Mass Input into the Process (kg)}}{\text{Mass of Desired Product (kg)}} = \text{E-Factor} + 1$$

5.2 Comparative Metric Analysis: Photoredox vs. Buchwald-Hartwig Coupling

Table 3 presents a comparative evaluation between classical Buchwald-Hartwig amination protocols and visible-light photoredox dual-catalyzed aminations (Yang et al., 2026).

Table 3: Comparative Sustainability and Process Metrics of Photoredox vs. Classical Buchwald-Hartwig Coupling

Process Metric	Classical Buchwald-Hartwig Coupling	Visible-Light Dual Photoredox Coupling	Green Chemistry Advantage / Impact
Reaction Temperature	80°C–140°C (Thermal heating)	20°C–30°C (Ambient LED)	Substantial energy reduction; protects thermally labile functional groups
Base Requirements	Stoichiometric strong base ($NaOtBu$, Cs_2CO_3, 1.5–2.0 eq)	Mild amine bases (t-BuNH$_2$, DABCO) or base-free	Prevents base-mediated substrate decomposition and racemization
Catalyst Loading & Precious Metal Content	1–5 mol% Pd + expensive phosphine ligands	0.1–0.5 mol% 4CzIPN / 1–5 mol% $NiCl_2$	Eliminates precious metals (Pd/Ir); lowers raw material costs
Process Mass Intensity (PMI)	High (150–300 kg/kg) due to aqueous workup	Low (30–80 kg/kg) in continuous flow	Reduces overall mass input, solvent footprint, and waste streams
Solvent E-Factor	Elevated; requires high-boiling polar solvents (DMF, Toluene)	Moderate to Low; compatible with MeCN, Acetone, Water	Lowers hazardous organic waste generation
Substrate Pre-functionalization	Requires Aryl Halides/Triflates ($Ar-X$)	Direct $C-H/N-H$ Cross-Dehydrogenative Coupling	Maximizes Atom Economy (AE); streamlines synthetic routes

This comparative breakdown demonstrates how photoredox amination resolves the major environmental and operational drawbacks of classical amination. Operating at ambient temperatures prevents thermal degradation, while utilizing Earth-abundant metal catalysts (Ni, Cu, Fe) or organic dyes reduces heavy metal contamination in Active Pharmaceutical Ingredients (APIs) below strict regulatory thresholds (< 10 ppm) (Halder, 2024).

5.3 Heterogeneous and Recyclable Photocatalytic Platforms

To further improve process sustainability, recent research has focused on immobilizing photosensitizers onto heterogeneous matrices. Heterogeneous platforms such as Porous Organic Polymers (POPs), Triazine-based Conjugated Microporous Polymers (CMPs), and flower-shaped Ru-doped ZnO nanoparticles enable catalyst recovery through simple filtration or centrifugation (Wang et al., 2023).

For example, carbon-nitride-based materials (e.g., CN-OA-m) paired with nickel salts promote red-light and solar-driven $C-N$ cross-coupling of aryl halides with pyrrolidines, pyrazoles, and anilines. These heterogeneous networks retain catalytic activity over multiple consecutive cycles without significant metal leaching, delivering target heterocycles such as tetracaine in up to 86% yield under solar irradiation (Zhao et al., 2018).

6. Challenges, Emerging Horizons, and Conclusions

6.1 Current Operational Bottlenecks

Despite rapid progress in visible-light photoredox-catalyzed $C-N$ bond formation, several operational challenges must be addressed to facilitate widespread industrial adoption:

1.**Attenuation of Light in Scale-Up (Beer-Lambert Law)**: Light intensity decreases exponentially with path length ($I = I_0 e^{-\epsilon c x}$), causing severe photon attenuation in large-scale batch reactors. This path-length dependence can

result in extended reaction times, catalyst degradation, or incomplete conversions when reactions are scaled beyond laboratory volumes (Hossain et al., 2019).

2. **Photochemical Catalyst Degradation**: High-energy excited states can undergo photobleaching or irreversible photodecomposition, reducing overall Catalyst Turnover Numbers (TON) and Turnover Frequencies (TOF) relative to thermal catalysts.

3. **Stereocontrol in $C(sp^3)-N$ Coupling**: Controlling absolute stereochemistry during the capture of open-shell, planar alkyl radicals by N-heterocyclic nucleophiles remains challenging, requiring specialized chiral Lewis's acid or chiral ligand dual-catalytic systems (Peña et al., 2025).

6.2 Emerging Horizons

To resolve these bottlenecks, several interdisciplinary strategies are currently being developed:

- **Microfluidic Continuous-Flow Photoreactors**: Flow chemistry reduces the optical path length to millimeter scale, ensuring uniform photon flux throughout the reaction medium. Continuous-flow processing increases throughput, eliminates batch-to-batch variability, and lowers process mass intensity.
- **Electrophotocatalysis**: Combining photoexcitation with an applied electrical bias (electrophotocatalysis) enables access to energetic redox states that are inaccessible via electricity or light alone. This dual strategy eliminates the need for stoichiometric chemical oxidants or reductants, yielding hydrogen gas as the primary byproduct.
- **Earth-Abundant Transition-Metal Dual Catalysis**: Replacing precious metal photosensitizers and cross-coupling centers with abundant metals like iron, cobalt, and copper reduces catalyst cost and environmental impact (Kumari & Singh, 2019).

Conclusion

Visible-light photoredox catalysis has fundamentally reshaped the synthetic landscape for constructing nitrogen heterocycles, offering a sustainable alternative to conventional thermochemical cross-coupling protocols. By converting low-energy photons into chemical potential through SET and EnT manifolds, photoredox systems generate highly reactive open-shell intermediates aminyl radicals, aminium radical cations, and carbon-centered radicals under exceptionally mild conditions. This review has demonstrated that both pure organophotoredox and dual metallaphotoredox architectures enable efficient C–N bond formation with remarkable chemo- and regioselectivity, facilitating the synthesis of privileged scaffolds such as indoles, quinolines, imidazoles, and pyrazoles. Comparative green chemistry analysis reveals that photoredox methodologies dramatically reduce E-Factors and Process Mass Intensity while eliminating precious-metal catalysts and stoichiometric strong bases, aligning with pharmaceutical industry imperatives for sustainable manufacturing. Despite these advances, challenges persist, including photon attenuation in scale-up, photocatalyst degradation, and stereochemical control in C(sp^3)–N coupling. Emerging solutions microfluidic continuous-flow reactors, electrophotocatalysis, heterogeneous recyclable platforms, and Earth-abundant metal dual catalysis offer promising avenues to overcome these bottlenecks. Future research should prioritize integrating these technologies with automated process optimization and expanding substrate scope toward complex, late-stage functionalization of bioactive molecules. Ultimately, visible-light photoredox C–N bond formation represents not merely a methodological alternative but a paradigm shift toward greener, more efficient, and economically viable synthesis of nitrogen heterocycles essential to human health and materials science.

REFERENCES

Beletskaya, I. P., & Averin, A. D. (2021). Metal-catalyzed reactions for the C(sp^2)–N bond formation: Achievements of recent years. *Russian Chemical Reviews, 90*(11), 1359–1396. https://doi.org/10.1070/RCR4999

Chen, J.-R., Hu, X.-Q., Lu, L.-Q., & Xiao, W.-J. (2016). Visible light photoredox-controlled reactions of N-radicals and radical ions. *Chemical Society Reviews, 45*(7), 2044–2056. https://doi.org/10.1039/C5CS00655D

Dorel, R., Grugel, C. P., & Haydl, A. M. (2019). The Buchwald–Hartwig amination after 25 years. *Angewandte Chemie International Edition, 58*(48), 17118–17129. https://doi.org/10.1002/anie.201904795

Feng, J., Xi, L.-L., Lu, C.-J., & Liu, R.-R. (2024). Transition-metal-catalyzed enantioselective C–N cross-coupling. *Chemical Society Reviews, 53*, 9560–9581. https://doi.org/10.1039/D4CS00102H

Heravi, M. M., Kheilkordi, Z., Zadsirjan, V., Heydari, M., & Malmir, M. (2018). Buchwald–Hartwig reaction: An overview. *Journal of Organometallic Chemistry, 861*, 17–104. https://doi.org/10.1016/j.jorganchem.2018.02.023

Kabir, E., & Uzzaman, M. (2022). A review on biological and medicinal impact of heterocyclic compounds. *Results in Chemistry, 4*, 100606. https://doi.org/10.1016/j.rechem.2022.100606

Prier, C. K., Rankic, D. A., & MacMillan, D. W. C. (2013). Visible light photoredox catalysis with transition metal complexes: Applications in organic synthesis. *Chemical Reviews, 113*(7), 5322–5363. https://doi.org/10.1021/cr300503r

Sinha, S., Singh, P. P., Kumar, D., & Srivastava, V. (2025). Recent advances in visible-light-driven photocatalytic synthesis of biologically active N-heterocycles. *Organic & Biomolecular Chemistry, 23*, 9993–10013. https://doi.org/10.1039/D5OB01411E

Vitaku, E., Smith, D. T., & Njardarson, J. T. (2014). Analysis of the structural diversity, substitution patterns, and frequency of nitrogen heterocycles among U.S. FDA approved pharmaceuticals. *Journal of Medicinal Chemistry, 57*(24), 10257–10274. https://doi.org/10.1021/jm501100b

Zhao, Y., & Xia, W. (2018). Recent advances in radical-based C–N bond formation via photo-/electrochemistry. *Chemical Society Reviews, 47*(8), 2591–2608. https://doi.org/10.1039/C7CS00572E

Corrigan, N., Shanmugam, S., Xu, J., & Boyer, C. (2016). Photocatalysis in organic and polymer synthesis. *Chemical Society Reviews*, *45*(22), 6165-6212.

Yang, Y. Y., Zhang, P., & Hadjichristidis, N. (2023). Two-photon excitation photoredox catalysis enabled atom transfer radical polymerization. *Journal of the American Chemical Society*, *145*(23), 12737.

Yadav, S., Singh, P. P., Murti, Y., Purohit, P., Singh, P. K., & Srivastava, V. (2024). Recent advances of 3DPAFIPN in photoredox catalysis. *Tetrahedron*, *163*, 134138.

Kancherla, R., Muralirajan, K., Sagadevan, A., & Rueping, M. (2019). Visible light-induced excited-state transition-metal catalysis. *Trends in Chemistry*, *1*(5), 510-523.

O'Brien, T. E., Morris, A. O., Villela, L. F., & Barriault, L. (2023). Synthetic applications of photochemically generated radicals from protic C (sp3)− H bonds. *ChemCatChem*, *15*(22), e202300989.

Cybularczyk-Cecotka, M., Szczepanik, J., & Giedyk, M. (2020). Photocatalytic strategies for the activation of organic chlorides. *Nature Catalysis*, *3*(11), 872-886.

Ni, J., Riyaz, B., Aamir, M., An, Z., Lu, Y., Muhammad, S., ... & Zhao, Y. (2026). From reagents to feedstocks: reprogramming heteroatom-containing molecules in modern organic synthesis. *Molecular Diversity*, 1-73.

Ghosh, T., Ahamed, S. S., Tastekin, S., & König, B. (2026). Cobalt in the Spotlight: Advances in Photocatalytic Cross-Coupling Reactions. *ChemPhotoChem*, *10*(8), e70243.

Dow, N. W. (2023). *New Photoredox Reactions Enabled by Unique Applications of Base Metal Catalysis* (Doctoral dissertation, Princeton University).

Goldschmid, S. L. (2025). *Metallaphotoredox Catalysis from Red to Blue: New Methods in C–N and C–C Cross-Coupling* (Doctoral dissertation, Columbia University).

Chen, J. R., Hu, X. Q., Lu, L. Q., & Xiao, W. J. (2016). Exploration of visible-light photocatalysis in heterocycle synthesis and functionalization: reaction design and beyond. *Accounts of chemical research*, *49*(9), 1911-1923.

Wang, F., Xie, X., Ye, B., Wang, L., & Zhu, B. (2026). Photocatalytic, Electrocatalytic, and Photoelectrocatalytic Radical-Mediated Three-Component Cascade Cyclization Reactions: Facile Access to N-Heterocyclic Compounds. *Advanced Synthesis & Catalysis*, *368*(4), e70306.

Liang, D., Zhou, Q. Q., & Xuan, J. (2024). Multiple-cycle photochemical cascade reactions. *Organic & Biomolecular Chemistry*, *22*(11), 2156-2174.

Azzi, E., Ghigo, G., Parisotto, S., Pellegrino, F., Priola, E., Renzi, P., & Deagostino, A. (2021). Visible light mediated photocatalytic N-Radical cascade reactivity of γ, δ-unsaturated N-Arylsulfonylhydrazones: a general approach to structurally diverse tetrahydropyridazines. *The Journal of Organic Chemistry*, *86*(4), 3300-3323.

Gilmore, K., & Alabugin, I. V. (2011). Cyclizations of alkynes: revisiting Baldwin's rules for ring closure. *Chemical Reviews*, *111*(11), 6513-6556.

Chadha, N., & Silakari, O. (2017). Indoles as therapeutics of interest in medicinal chemistry: Bird's eye view. *European Journal of Medicinal Chemistry, 134*, 159–184. https://doi.org/10.1016/j.ejmech.2017.04.003

Ghosh, S., Rana, G., Kar, A., Sahoo, R., & Jana, U. (2025). Visible-light-triggered organophotoredox-catalyzed oxidation of 3-(benzylidine)indoline to indole-3-carbinols and 3-acyl indoles. *Organic & Biomolecular Chemistry, 23*(23), 5643–5656. https://doi.org/10.1039/D5OB00401B

Kumari, A., & Singh, R. K. (2019). Medicinal chemistry of indole derivatives: Current to future therapeutic prospectives. *Bioorganic Chemistry, 89*, 103021. https://doi.org/10.1016/j.bioorg.2019.103021

Talvitie, J., Mollar-Cuni, A., Nyman, J., Koivula, J., Hendrickx, L., Muñoz Rodríguez, P., & Helaja, J. (2025). Photoredox catalytic synthesis of indoles via direct N–H activation to generate putative aminyl radicals. *Organic Letters, 27*(37), 10537–10541. https://doi.org/10.1021/acs.orglett.5c03410

Zard, S. Z. (2008). Recent progress in the generation and use of nitrogen-centred radicals. *Chemical Society Reviews, 37*(8), 1603–1618. https://doi.org/10.1039/B714270B

Borah, P., Borah, P., & Moon, L. E. (2026). Green and Sustainable Approaches in Multicomponent Reactions: Solar Energy, Ultrasound, Solid-Phase, and Photochemical Methods: A Review. *ChemistrySelect*, *11*(35), e74420.

Salah, A. R. M. (2025). Photochemistry in Organic Reactions: Mechanistic Pathways and Green Applications.

Lee, K., Han, S., Kim, M., Kim, B. S., Park, J. A., Lim, K. S., ... & Kim, H. O. (2025). Metal–Organic Framework for Plastic Depolymerization and Upcycling. *Crystals*, *15*(10), 897.

Yang, C. J., Wang, X. Y., Zhu, M. Q., Zhao, T., Pan, Y. Z., Dou, Y., ... & Wang, D. (2026). A Panoramic View on Plastic Waste Recycling and Upcycling: Heterogeneous Catalytic Strategies for Diverse Plastics and Multiple Pathways. *Advanced Materials*, *38*(35), e21912.

Halder, R. (2024). *Late-stage aromatic C— H difluoroalkylation and amination $ via $ arylthianthrenium salts and $^ 18} $ F-labeling of peptide $ via $ ruthenium-mediated deoxyfluorination* (Doctoral dissertation, Dissertation, RWTH Aachen University, 2024).

Wang, Y., Yang, Y., Deng, Q., Chen, W., Zhang, Y., Zhou, Y., & Zou, Z. (2023). Recent progress of amorphous porous organic polymers as heterogeneous photocatalysts for organic synthesis. *Advanced Functional Materials*, *33*(51), 2307179.

Zhao, S. N., Wang, G., Poelman, D., & Van Der Voort, P. (2018). Metal organic frameworks based materials for heterogeneous photocatalysis. *Molecules*, *23*(11), 2947.

Hossain, A., Bhattacharyya, A., & Reiser, O. (2019). Copper's rapid ascent in visible-light photoredox catalysis. *Science*, *364*(6439), eaav9713.

Peña, L. F., Parte, L. G., Díez-Poza, C., Guerra, J., & López, E. (2025). Homogeneous catalysis in continuous flow integrating photocatalysis, electrocatalysis, and automation technologies. *Communications Chemistry*, *8*(1), 336.

IEER
Institute for Excellence in Education & Research